Use of THz reflectometry for roughness estimations of archaeological metal surfaces

***Ilaria Cacciari*[1,*], *Salvatore Siano*[1]**

[1]*Institute of Applied Physics "Nello Carrara"*
Via Madonna del Piano 10, 50019 Sesto Fiorentino (FI), Italy
**i.cacciari@ifac.cnr.it*

Abstract: In this work, using a time domain spectrometer, we have investigated the reflection of THz pulses from surfaces that exhibit a variable degree of roughness. The study was mainly aimed at assessing the influence of the surface texture on the amplitude and shape of the pulses reflected by stratified materials, and at exploring the potential of this technique for achieving quantitative information on the roughness of the material interfaces hit by the THz beam. The behaviour of the reflected THz pulses was investigated by considering angular measurements on a set of suitable mock-ups. Measurements were carried out on an authentic archaeological Roman coin that exhibited different corrosion situations. An electromagnetic model was used for estimating the roughness of outer and inner surfaces. The comparison of the results with those provided by other techniques made it possible to parameterise the surface texture such as the traditional contact micro-profilometry and the more recently used 3D digital microscopy.

Keywords: THz Time Domain Spectroscopy, reflectometry, roughness, scattering mean power, corroded metal

1. Introduction

During the last decades, the potential of THz waves has been thoroughly explored in several fields, including fundamental disciplines such as physics and chemistry and a number of application contexts where they have been tested for tomographic and compositional characterizations. Some of these applications, for example those concerning security, have undergone relevant applicative developments and spreading, whereas in many other cases THz spectroscopy is still far from the current practices and basic insights are needed.
THz waves can answer questions regarding material characterization that have been left unsolved by complementary techniques such as Vis-NIR optical microtomography, which can only be used for thin translucid material layers (Optical Coherence Tomography) or Vis-IR imaging, which is not able to recognize the difference between inner material interfaces, or Vis-IR spectroscopy, which cannot provide compositional information on disguised material layers.
Thus, there are two main appealing [1] features that stimulate a continuous increase in studies on the THz approach: THz waves can penetrate dielectric materials, with thickness ranging from some tens of microns to some millimeters, and can identify them from their spectral signature.
Thus for example, in automotive industry the thickness of multi-layer paintings can be accurately measured [2, 3] using THz spectroscopy in order to assess whether adjacent layers are detached, which is an important piece of information since to work properly protective coating should not penetrate the inner painting. In medicine, cancer diagnosis by means of THz imaging has recently been demonstrated with both ex-vivo and in-vivo images [4]. In construction and building industry, manufacturing imperfections and internal structures can be visualized with THz waves [5]. There the technique has been proposed for testing existing insulating layered structures, as well as for developing novel materials characterized by higher performances [6]. The potential of THz waves appears even more intriguing in the field of cultural heritage where the variety of materials and state of conservation should be known by restorers and curators in order to allow them to decide the best conservation strategy [7-9]. In this field, there are successful examples of characterization of paint layers [10, 11], parchment and papyrus manuscripts [12, 13], whereas only preliminary works were reported on archaeological metal surfaces [14, 15].
Since the modulations of the latter often fall in the order of magnitude of the THz wavelengths (typically from mm down to μm), the reflected pulses can be significantly attenuated and altered by surface scattering. This effect can result in serious limitations for the tomographic characterization of corroded archaeological metal artefacts but, at the same time, it can be exploited for collecting micromorfological data on the surfaces under study. To this end, the main challenge is to correlate the THz reflected pulses to the surface texture parameters and then (in perspective) to its state of conservation. Following a preliminary study, in which the possibility of detecting the presence of a metal surface beneath thick corrosion layers was investigated, here, further insights on the potential of THz analysis for characterizing archaeological artefacts are reported. In particular we investigated the possibility of extracting information on the surface roughness of outer and inner surfaces from THz reflectometry. To this aim, samples of different roughness were prepared using a set of abrasive paper samples. These were successfully characterized using the Beckman-Spizzichino (BS) [16, 17] then the method was validated on a heavily corroded silver alloy Roman coin.
The use of abrasive papers as roughness standards for THz measurements was proposed by some authors [18-20]. In [18] sandpaper was used as it is, thus neglecting the effects of the specific material superposition (grains, glue, and paper) and

associated multiple scattering contributions. These were prevented in [19] with copper coating while in [20] sandpaper was used in order to impress its roughness on a pellet of lactose. Here, gilded sandpaper samples were used.
The applicability of the BS model to the THz reflectometry was shown in [21] by comparing the texture parameters provided by the theory with the roughness measurements carried out using the confocal microscopy. In this study, which was carried out in order to estimate the effects of diffuse reflection in indoor THz links, the validity of the mentioned BS model for diffuse THz scattering from plaster and wallpaper surfaces was verified. Similar comparisons between roughness parameters derived from the theory and those directly measured were also reported in [18] and [20]. Moreover, the use of the BS model was exploited in previous works in order to study the relation between the frequency, reflectivity, and roughness of conductors [22], the refractive index and thickness of ceramic coating on metal substrate [23], spectral feature of rough dielectric materials [20, 24]; and reflectivity of optically thick building materials [25].
Here, after optimizing the angular configuration that maximized the reflected signal, the validity of the BS model was demonstrated once again in the THz range through a systematic characterization of the mentioned gilded sandpapers. Moreover, this work reports the first application of THz Time Domain Spectrometry (TDS) in order to estimate the roughness parameters of both outer and inner interfaces of a material layer. The results achieved were congruent with the corresponding ones measured using standard profilometry and 3D digital microscopy. Finally, the surface roughness of the corroded Roman coin mentioned above was successfully carried out using the BS method. The extension of the use of the THz reflectometry to the estimation of interface roughness represents an enrichment of the present approach that can stimulate its use in study and conservation of the metal heritage.

2. Materials and methods

A THz Time Domain Spectrometer (TDS) was used in the present study [26, 27]. This pulsed system was equipped with a 70 fs fiber laser source operating at 1550 nm exciting two photoconductive antennas (PCA) via fiber optic, whose emission spectra was between 0.1-1 THz (0.3-3 mm corresponding wavelength range). The two PCAs were used for THz generation and detection in reflection geometry. The THz pulse was focused with a Teflon lens (f=30 mm) on the sample at an incident angle θ_i with respect to the normal direction, and the reflected signals were collected at different angles (θ_r) using a goniometer and focusing optics. In order to measure the spot size, we considered a Gaussian beam and the edge technique; a spot of about 1.2 mm was measured at 1/e amplitude attenuation. A very good reproducibility of THz parts alignment was achieved with this setup. This instrument was used to characterize several samples described hereafter in some details.

2.1 Samples

The effect of surface texture on THz reflection measurements was systematically studied using a set of prepared samples then, a real corroded archaeological object was characterised. The former were devised in order to achieve a reasonably homogeneous surface textures in the mm size range. For this purpose, abrasive sheets presenting spatial modulations within the order of magnitude of the wavelengths corresponding to the THz spectral range were considered. Conventionally speaking, abrasive papers are named according to ISO Grit standards with “Pn”, where “n” is the number of lines/inch of the sieve used, which corresponds to a similar amount of sharp particles/inch^2 and to a specific average size (f.i. P40 indicates 40 lines/inch and an average size of 438 µm)
Even if in most cases the manufacturer does not declare the roughness degree [28] it is important to keep in mind that the fabrication process guarantees only that the mean grain size is relatively constant and, therefore, reproducible according to ISO standards. This could be interpreted as a relatively constant roughness degree that should be measured.
Five pieces of abrasive paper measuring about 1 cm^2, with average grains size ranging between 82-425 µm (P180-P40) were used (3M™ 314D series). All the information provided by the manufacturer was reported in tab. 1. Since the work was focused on the investigation of the dependence of the reflected temporal profile of the THz pulse, multiple reflections from the particle interfaces and the back surface of the paper were avoided by the metallization of the front surface of the samples. They were coated with a thin layer of gold that was sputtered by means of a typical glow discharge device (EMITECH K550X) used for the preparation of samples for SEM examinations. Moreover, a flat polished glass plate was sputtered together with the abrasive paper samples, and this was used as reference mirror.

Tab. 1. Abrasive papers used for the preparation of samples.

314 D series	ISO Designation	Average Grain Diameter (μm)
Coarse	P40	425
Medium	P80	201
Fine	P100	162
Fine	P120	125
Very fine	P180	82

The layer thickness was selected according to the skin depth of penetration for a conductor [29, 30]:

$$\delta = \sqrt{\frac{\rho}{\pi f \mu_0 \mu_r}} \qquad (1)$$

where ρ is the resistivity of the metal to be sputtered (Ω m), f is the frequency (Hz), with μ_0 the permeability constant and μ_r the relative permeability [31]. For gold ρ=2.24 $\cdot 10^{-8}$ Ω m and μ_r=1 [32] skin depths of 75 and 238 nm are obtained at 1 THz and 0.1 THz respectively. Thus a gold layer of about 200 nm was sputtered by controlling both the current and the deposition duration. This value was considered adequate for the present study because it prevented any absorption effects in the 1-0.1 THz range. In other words, all the THz energy was reflected at the surface and volume scattering could be considered as negligible. The THz pulse shape and amplitude were influenced, therefore, only by the texture of the outer surface, which was carefully characterised by means of surface texture measurements (see below).
We also considered more complex systems such as dielectric layer on metal. An acrylic paint layer was applied on the gilded abrasive paper, thus achieving a very smooth outer interface (air/paint). In this way the THz pulse experienced two reflections (Fig. 1), and was attenuated by absorption and multiple scattering of the paint layer.

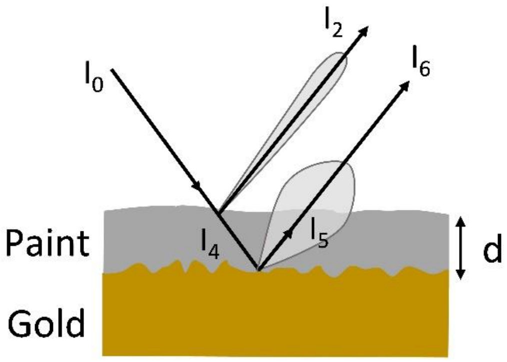

Fig. 1 Paint layer on gilded rough surface: part of the incident pulse (I_0) is reflected at the outer interface (I_2), and part travels in the paint layer, the pulse I_6 results attenuated by scattering at the inner interface and by propagation in the absorbing medium.

After the systematic investigation carried out on the laboratory samples as described above, a silver alloy Roman coin (an Antoninianus, AD 230-260) was characterized using THz TDS. This finding was mostly stratified and corroded, while its silver alloy substrate was recognizable in a relatively small shining area (Fig. 2). There was no information available regarding the state of the bulk beneath the stratification.

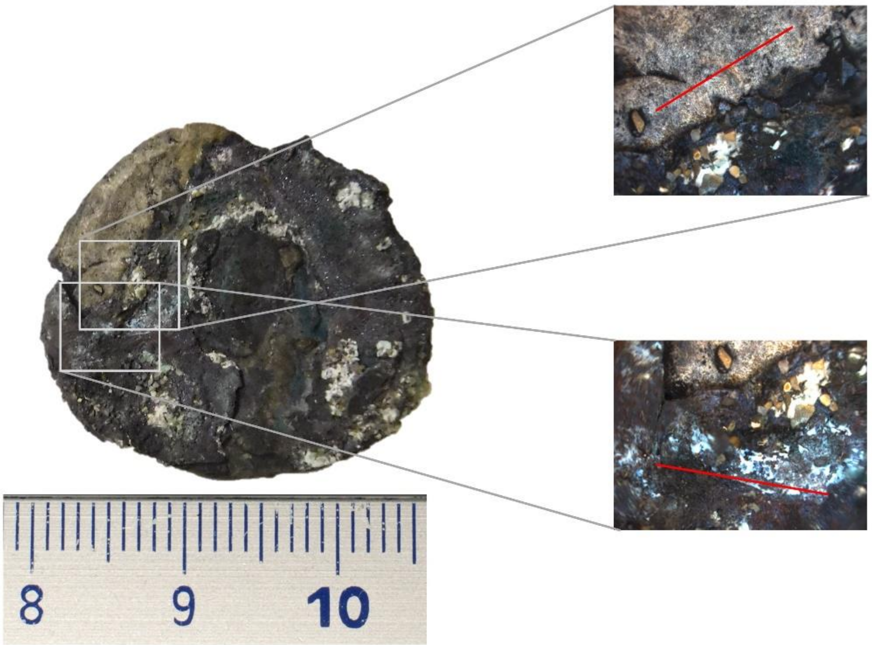

Fig. 2. Left) Roman corroded coin. Right) investigated sites, the height profiles were extracted from red lines. The scale is expressed in cm.

2.2 Surface texture characterization

In order to achieve numerical evaluations of the surfaces understudy to be associated the THz investigation, texture parameters were measured with both optical and mechanical devices. Standard roughness parameters and the correlation function were considered, which parameterized profile and surface modulation, respectively.

Generally, the height coordinate of the surface is mathematically expressed as a random function of the coordinate xy. The shape of the surface is then determined by the probability distribution of the height coordinate. A number of amplitude parameters can be extracted from the height distribution. The most commonly used ones are the mean (R_a) and the root mean squared (R_q) roughness, which are usually expressed in micrometers [33]. The former is defined as the arithmetical average of the absolute values of the profile height deviation from the mean line. R_q calculates the root mean square average of the profile height deviations from the mean line (i.e. the standard deviation of the height distribution) recorded within the measurement length. The latter is selected in order to include enough small irregularities for a meaningful calculation while excluding unimportant long-wavelength components. Guidelines for the selection of the measurement length are provided in the ISO 11562 standard; in the present study, a sampling length of 4.8 mm was selected.

The statistical distribution of heights does not provide information about the distances between the peaks and valleys, and these could be provided by the autocorrelation length (τ). This is defined as the horizontal distance at which the autocorrelation function decays permanently to a certain minimum value: in the case of normally distributed surfaces, to 1/e [34].

The above described parameters were derived from height maps and profiles as measured using a 3D microscope based on the "shape from focus" technique [35, 36] and a commercial diamond stylus micro-profilometer. In the latter case, ten profiles were measured for each sample by setting a scan length of 4.8 mm, then considered the average texture parameters (R_q, τ) and the maximum deviation as the error. By using the imaging approach to the roughness measurement, a 6.4×6.4 mm 3D model was reconstructed for each sample. From the 3D reconstruction, ten profiles (4.8 mm length) were extracted along different directions and the texture parameters were calculated to enable comparison with micro-profilometer results.

2.3 Background: effect of roughness on backscattering

Light incident at the interface between two different media is reflected according to well-known laws. In general, an estimate of the surface roughness parameters using reflectance measurements can be achieved following two different approaches: undulatory or geometrical optics. The latter represents a suitable simplification whenever the wavelength is

small as compared to the typical sizes of the system understudy. However, since in the present case the wavelengths were of the same order of magnitude of the spatial modulations of the sample surfaces, the former approach must be used
As anticipated above a description of the behavior of THz pulses reflected by rough surfaces can be based on the Beckman and Spizzichino (BS) model [16]. The mean power (P_s, square amplitude of the electric field) scattered by a rough surface, whose heights were normally distributed with standard deviation R_q, and correlation distance τ, is given for the mono dimensional case by:

$$P_s = e^{-g}\left(sinc(vL) + \frac{\sqrt{\pi}F^2\tau}{2L}\sum_{m=1}^{\infty}\frac{g^m}{m!\sqrt{m}}e^{-\frac{v^2\tau^2}{4m}}\right), \quad (2)$$

where θ_i and θ_r are the incidence and reflection angles respectively,

$$\sqrt{g} = 2\pi\frac{Rq}{\lambda}(cos\theta_i + cos\theta_r) \quad (3)$$

$$v = \frac{2\pi}{\lambda}(sin\theta_i - sin\theta_r) \quad (4)$$

$$F = sec\theta_i\frac{1+\cos(\theta_i+\theta_r)}{cos\theta_i+cos\theta_r} \quad (5)$$

where L is the spot size, and m an integer number. The dependence of the mean power scattered on g, τ, and v can be studied according three scenarios: $g<<1$, $g\approx1$, $g>>1$. Since $\sqrt{g}$ is proportional to the roughness, these three cases correspond to a slightly, moderately and very rough surface. In the specular direction $\theta_i=\theta_r$, and for any roughness value, v=0 and F=1 were obtained. The roughness R_q can be extracted from the scattered mean power in the specular direction providing the wavelength, and the correlation length, but in practice, its measurement is not straightforward [37]. The formulae above are applicable rigorously in case of a plane wave incident on a rough surface, and must hence be considered a first approximation in practical cases.
For each samples considered here, the mean power scattered in the specular direction was measured and then R_q was extracted from Eqs. 2-3. These roughness values were finally compared with those provided by digital microscopy and contact micro-profilometry.

3. Results and discussion

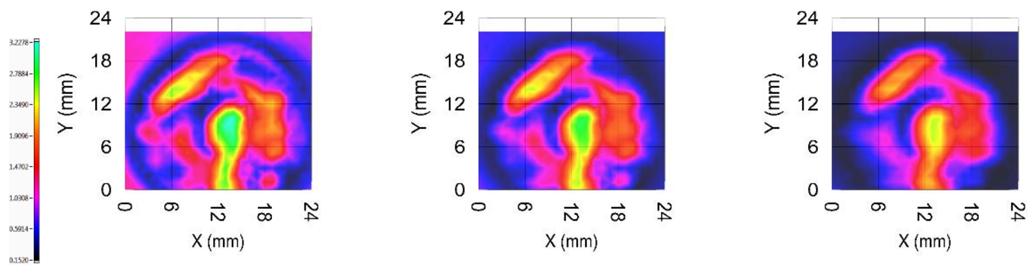

Fig. 3. THz Imaging of a Roman coin in specular geometry at incident angle 30° (left), 40° (middle) and 50° (right). The colour scale is in a.u..

One of the main aims of this paper was to prove the ability of THz to image real archaeological surfaces with a different roughness degree. The first consideration to be done was about the setup geometry. The goniometer introduced in the setup enabled us to perform several angular measurements. In particular, with the sample fixed in a position, two situations were considered: in the first case in specular geometry, we varied the incident angle; in the second case we fixed the incident angle and varied the detection angle. These angular measurements were performed in order to study the most favourable geometry [38]. In the first case, we observed a strong decrease in the THz reflected signal as the incident angle grew. We thus chose as the incident angle, the mimimum permitted by geometrical constraints of the setup (30° to the normal to the sample surface). In Fig. 3 was reported the THz imaging of a real corroded Roman coin in specular geometry: the incident angles were 30°, 40° and 50°. Each pixel represented the peak-to-peak amplitude of the THz reflected pulse. The peak to peak amplitude decreased with an increase in the incident angle, thus the dark areas expanded. In the second case, at the incident angle of 30°, the reflected amplitude was measured at angles in the 30°-50° range at 5° step. As expected, the maximum THz reflected signal was obtained in the specular geometry.

Once the appropriate THz geometry (specular reflection at 30°) was selected, five pieces of abrasive papers were considered for THz measurements. They were gilded by sputtering. The deposited layers were observed under an electron scanning microscope; the original surfaces were completely covered and they appeared uniformly gilded. This was important in order to guarantee that the volume scattering would be negligible.

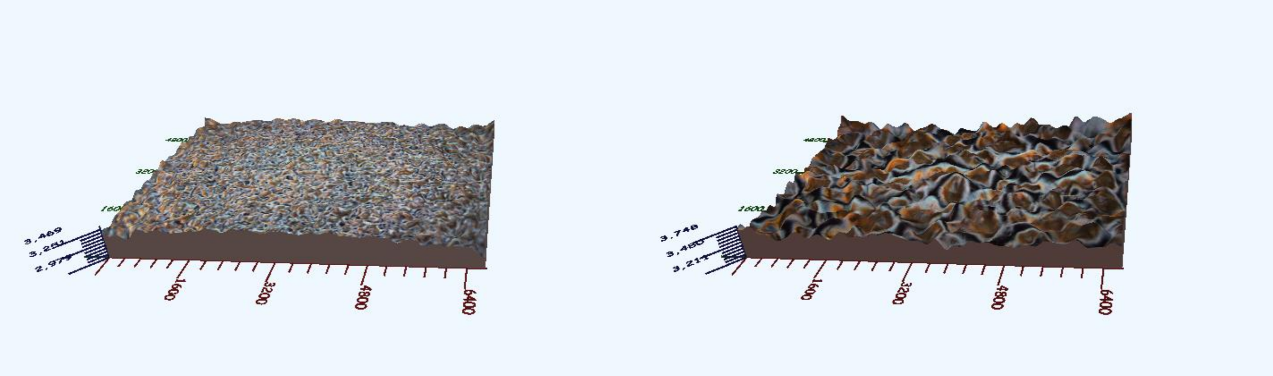

Fig. 4. 3D reconstructions of two gilded abrasive papers: left) P180, right) P40. The vertical scales are expressed in mm.

As mentioned above, the roughness of the gilded samples was measured using independent techniques: micro-profilometry (A) and 3D microscopy (B) through average processes. The results were reported in Tab. 2, while Fig. 4 displayed two examples of the 3D reconstructions of the prepared samples. As expected, the higher roughness degree corresponded to the low grit size designation, while the very good agreement between the results of the two techniques was rather surprising [36].

Tab. 2. R_q measured using contact profilometry (A), R_q and τ measured with 3D microscopy (B).

	R_q (μm)		τ(μm)
	A	**B**	**B**
P40	69±10	71±9	296
P80	65±6	62±8	293
P100	57±13	57±9	291
P120	49±11	46±9	288
P180	38±10	36±9	121

The height distribution from each profile was calculated by using a normal distribution. It was observed that both the slightly and moderate rough cases could be fitted very well with this distribution, in these cases the goodness of the fit was measured by a R^2 value near 1. On the other hand, for the rough case, the normal distribution could not be used and the R^2 decreased. These two extreme situations (P180 and P40) were represented in Fig. 5.

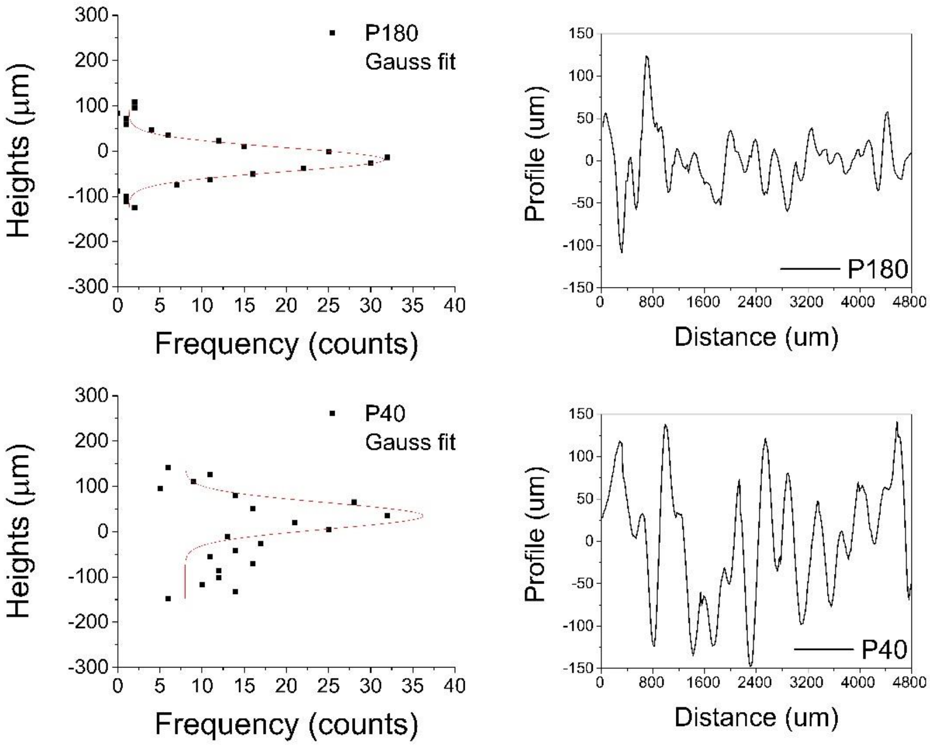

Fig. 5. Histograms of the Gaussian distribution of heights extracted from a height profile of P180 (top) and P40 (bottom), R^2 is 0.98 and 0.13 respectively.

The normal distribution was not the most suitable distribution for all the samples. Nonetheless, the correlation length was calculated (Tab. 2) with an error of about 10%, which was estimated by repeating the measurements for all the profiles considered. However, the lack of Gaussian distribution for coarse and medium grit sizes makes the values found of limited meaning.

Each gilded abrasive paper was placed in the THz TDS and kept in a constant position during the measurements. It was observed that with rougher surface less THz signal was reflected. For each sample, we repeated the measurement of the reflected THz pulse on different points. With this procedure, the stability of the system was monitored and the sample uniformity was controlled. The error obtained ranged from about few percent in the very fine (P180) to 15% with rougher sample (P40).

For each sample, the amplitude of the THz pulses reflected at different angles, were normalized at its maximum value, and bell-shaped functions were fitted (Fig. 6). Interestingly, the measured FWHMs linear increased with the roughness value. This could be explained qualitatively by considering the transition from specular reflection to diffuse scattering. For very fine samples (P180), a narrow side lobe around the specular direction was reflected: in this case the specular components dominated. For fine and medium surfaces (P120-P80), the reflection lobe tended to lose its pronounced orientation and the diffuse components emerged.

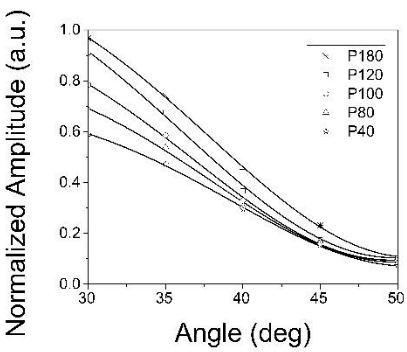

Fig. 6. Normalized THz peak amplitude vs reflection angle.

THz reflected waveforms were deconvoluted as described above, then the measured mean scattered power P_s was used to derive g and therefore R_q from Eqs 2-3. Since the peak of the THz band used (Fourier Transform of the incident pulse) was at 0.2 THz, we put λ=1500 μm in Eq. 3. The approximation g<<1 was considered since 0.07<g<0.26 for the roughness range of Tab. 2. In this case, the series in Eq. 2 converges very quickly thus allowing its approximation with the first term of the sum. This, along with the first order approximation of the exponential factor, allows deriving the estimation of R_q analytically:

$$P_s \cong 1 + g \cdot \left[\frac{\sqrt{\pi}\tau}{2L} - 1\right], \qquad R_q \cong \frac{\lambda}{2\pi\sqrt{3}}\sqrt{\frac{2L(P_s-1)}{\sqrt{\pi}\tau-2L}}. \qquad (6)$$

Here, $L\cong 1.2$ mm was measured thus, according to Tab. 2, $\tau/L \leq 0.25$, which made g almost independent on τ. This condition is equivalent to neglect the sum term in Eq. 2 when $L >> \tau$, which provides $P_s \cong e^{-g}$. This simplified expression for roughness estimations was used in [18].

The comparison between R_q derived from the theory and those measured (Tab. 2) is shown in Fig. 7. In the cases of relatively fine grain (P180-P100) R_q values were below 55 μm and the agreement was satisfactory, while in the medium and coarse cases (P80, P40) significant differences were found. This was due to the BS assumption's not being fulfilled by the two latter samples: the height distribution in this case could not be fitted with a normal distribution. Moreover, it should be noted that the R_q value from which the BS model predicted well P_s (i.e. below 60 μm) corresponds to R_q defined by the Fraunhofer criterion [20], $R_q < l/32\cos\theta$, which provides for a wavelength of 1500 μm and an incident angle of 30°, R_q = 54 μm. Thus, for the present application the validity condition of the BS model corresponds to the limit of moderate scattering regime.

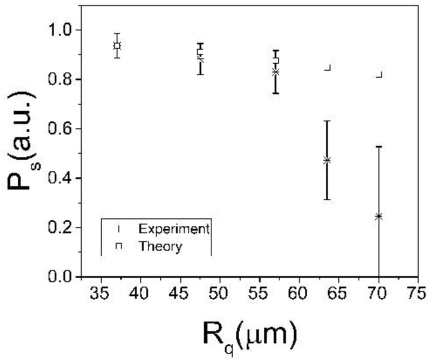

Fig. 7. Mean power scattered by the gilded samples in specular geometry: theoretical and experimental comparison.

Roughness measurements were also carried out on a more complex system: paint layer on gilded abrasive papers. In this case, a number of pulses were observed in specular geometry. In Fig. 8 the measured waveforms for the painted samples P180 and P120 are displayed along with the corresponding deconvolutions. The latter were calculated according to the method reported in [39]. For both samples the first two peaks are ascribable to the air/paint and paint/gold interfaces, while the others are interpretable as a result of the etalon effects introduced by the paint layer [40].

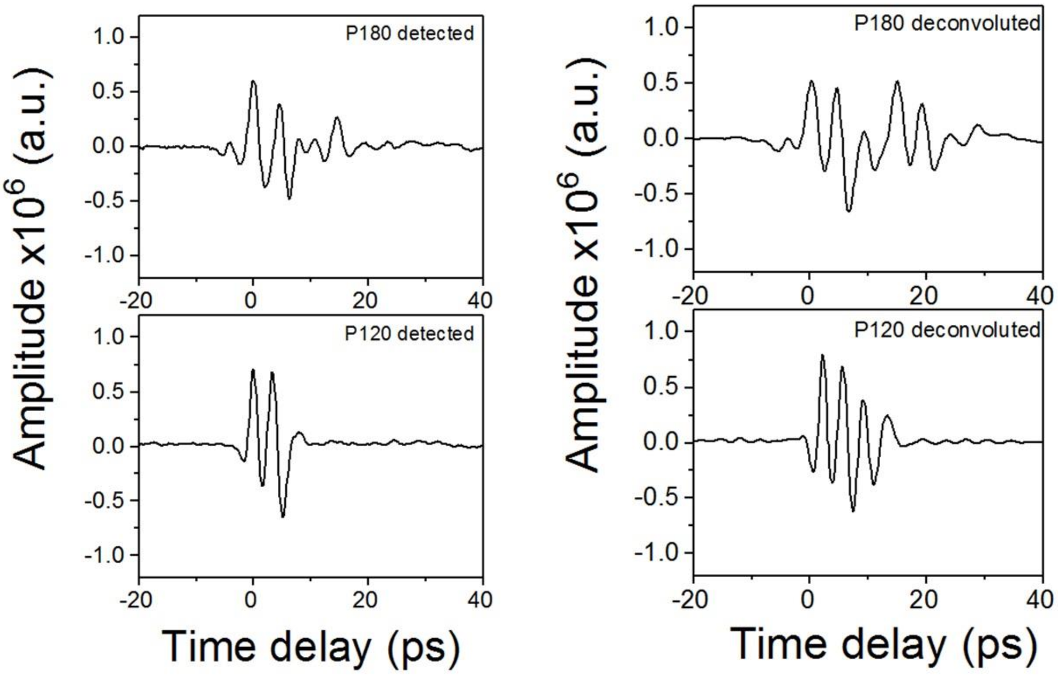

Fig. 8. Paint layer on gilded sandpaper surface: left) reflected THz pulses for P180 (up) and P120 (down); right) deconvoluted reflected waveforms for P180 (up) and P120 (down).

The reflection from the mentioned painted samples were compared with that from a flat and smooth gold surface (used as a reference mirror) in order to extract information on the roughness of the inner interface. In both cases, the same thickness of a few hundred of microns was considered. Thus, both the real (n) and imaginary (k) part of the refractive index of the paint were calculated from reflection measurements according to Kramers-Kronig relations. At 0.2 THz n=2.16 and k= 0.16 were achieved. In particular, the real part of the refractive index was compatible with acrylic paint group refractive index reported in the literature [3].

Once the imaginary part of the refractive index was known [41], in the model sketched in Fig. 1, the absorption loss introduced by propagation in the paint layer (I_4) was estimated by means of simulation. In this case, the Fresnel coefficient for perpendicular polarization, and absorption introduced by propagation were used in order to evaluate the signal that hits the detector (I_6). We assumed that the mean scattered power P_s was the ratio I_6/I_4. It was found for sample P180 P_s=0.943, thus R_q=35 and for sample P120 Ps=0.896 thus R_q = 48 μm. The calculation has been repeated with the deconvoluted signals: for sample P180 it was found P_s=0.937, thus R_q=37 μm and for sample P120 Ps=0.906 thus R_q = 51 μm. These values were compatible with the measurements of the gilded abrasive paper without paint layers.

Finally, roughness measurements were carried out also on the Roman coin described above. Two areas apparently exhibiting different roughness were selected, within the stratified and metallic zone, respectively (see the rectangles in Fig. 2). The corresponding mean scattered power of the outer surface of the former zone was slightly less than that of the uncovered metal (Fig. 9). By considering the same L and λ taken into consideration for the abrasive papers, we derived roughness estimations (R_q) of 80±2 and 117±4 μm, respectively. The error was estimated by changing the correlation length in the 100-200 μm range.

Although in principle, as shown above for the painted abrasive paper sample, the roughness estimate for encrusted metals could be extended to the second possible interface between the mineral stratification and metal substrate, in practical cases this seems rather hard. To date we have investigated several archaeological artefacts presenting deep corrosion phenomena and the internal reflections were detected only in relatively a few cases. This was due to various possible attenuation causes of the THz beam including local absorption by metal minerals and trapping within the intergranular and transgranular corrosion. On the other hand, when reflections from internal interfaces are detected the waveforms are often rather complex because of the material stratification. Figure 10 shows the detected reflection from outer and inner interfaces of a corroded zone of the present ancient coin, along with the corresponding deconvolution [39]. As shown, three main peaks were detected associated to the outer surface, mineral-mineral interface, and mineral-metal interface, respectively. Similarly to the prepared samples, the latter peaks could be exploited for roughness calculations if data on of the refraction indexes are available. For the present silver and copper minerals stratification we have not sufficient data for reliable estimations. Nevertheless, the deconvoluted waveform of Fig. 10 provided evidence of a double layer mineral stratification and of the presence of the metal substrate underneath.

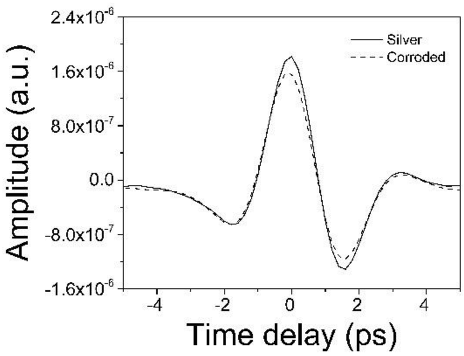

Fig. 9. THz pulses reflected from metallic and mineralized areas, respectively, of the Roman coin.

The same areas analysed with THz were studied with 3D digital microscopy, by reconstructing height maps and calculating the root mean squared roughness. R_q=115 and 69 μm were found for mineralized and metallic surfaces, respectively. The corresponding roughness values derived using THz reflection measurements were in good agreement only for the former site and metallic zones, respectively.

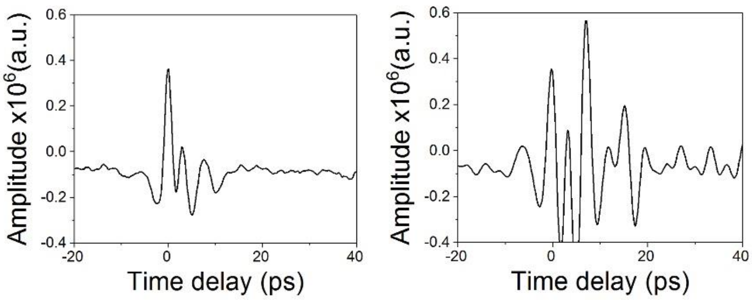

Fig. 10. THz reflections from a stratified zone on the Roman coin: left) detected signal; right) deconvoluted signal.

4. Conclusions

In this work we explored the potential of THz reflection measurements in order to derive quantitative information on the surface roughness of single or multilayer systems using the Beckman-Spizzichino scattering theory. Despite the fact that such a model was strictly true for a plane wavefront and normal distribution of the surface heights, the results achieved showed that the lack of the former conditions did not completely affect the relation between surface roughness and mean scattering power that it provides. Conversely, the presence of a normal distribution is crucial for the exploitation of the method.

Reflection measurements were performed on prepared samples of different roughness and a Roman coin. The root mean squared roughness, derived from the aforesaid theory was compared with the corresponding ones directly measured using a contact profilometer and calculated by means of 3D digital microscopy, respectively. A very good agreement was achieved for abrasive papers thinner than P100, which presented almost normal height distributions. Very interestingly, the roughness measurements carried out on the ancient coin using the scattering model and 3D imaging also provided congruent results. The best agreement (as for the abrasive papers) was achieved in the case of normal height distribution, but even in the case of not normal distribution, the results obtained are not completely out of range and can be useful as an order of magnitude. Thus suggesting that the condition of normal height distribution is not really limiting.

This proves that, in addition to tomographic and spectroscopic information, THz reflectometry can also be exploited for quantitative calculations of the surface roughness. Such a feature becomes particularly interesting whenever a roughness estimate can be extended to surfaces beneath the outer one. This possibility has been successfully demonstrated in this study on prepared samples and it could be exploited in comparative measurements associated with conservation treatments (ex. to compare the roughness parameter before and after cleaning using different material removal techniques). It is also

important to underline that, as explained in the text, R_q is here derived from single spot-reflectometry, which is something much more practicable in concrete applications than tomographic imaging requiring very long measurement times.
Further studies will be dedicated to extend the approach proposed to a variety of surface texture measurement needs, within the characterization of the state of conservation and the assessment of conservation treatments carried out on a variety of artefacts of historical and artistic interest.

5. Acknowledgement

The present work was carried out within the project IPERION CH (H2020-INFRAIA-2014-2015, Grant No. 654028). The authors also acknowledge the financial support of the "*Fondo per le infrastrutture produttive*", of the Tuscany Region (D.G.R.T. n. 924 - 19/10/2009) for the purchase of the THz instrument used in the present study.

References

[1] K. Lewotsky, "Terahertz's penetrating appeal", SPIE Professional Magazine, April 2006 DOI: 10.1117/2.4200604.06
[2] S. Krimi, J. Klier, J. Jonuscheit, G. von Freymann, R.Urbansky, and R. Beigang, "Highly accurate thickness measurement of multi-layered automotive paints using terahertz technology", Appl. Phys. Lett. vol. 109, pp. 021105-1(4), 2016.
[3] T. Yasui, T. Yasuda, K.-ichi Sawanaka, T. Araki, "Noncontact Terahertz Paintmeter for Real-Time Two-Dimensional Cross-Section Imaging of Paint Film Thickness", Proc. 9th European Conference on Non Destructive Testing, pp.1-4, 2006.
[4] S. J. Oh, Y. Huh, J. Suck Suh, J. Choi, S. Haam, J. Son, "Cancer Diagnosis by Terahertz Molecular Imaging Technique", Journal of Infrared, Millimeter, and Terahertz Waves, vol. 33, no. 1, pp 74-81, 2012.
[5] A. Abina, U. Puc, A. Jeglič, A. Zidanšek, "Applications of Terahertz Spectroscopy in the Field of Construction and Building Materials", Applied Spectroscopy Reviews, vol. 50, no. 4, pp. 279-303, 2015.
[6] A. Abina, U. Puc, A. Jeglič, A. Zidanšek, "Structural characterization of thermal building insulation materials using terahertz spectroscopy and terahertz pulsed imaging", NDT&E International, vol. 77, pp. 11-18, 2016.
[7] K. Fukunaga, "THz Pulsed Time-Domain Imaging (THz Pulsed TDI)" in THz Technology Applied to Cultural Heritage in Practice, Springer Japan, 2016.
[8] A. Cosentino, "Terahertz and Cultural Heritage Science: Examination of Art and Archaeology", Technologies vol. 4, no. 6, pp. 1-13, 2016.
[9] J. B. Jackson, J. Bowen, G. Walker, J. Labaune, G. Mourou, M. Menu, and K. Fukunaga, "A Survey of Terahertz Applications in Cultural Heritage Conservation Science", IEEE Trans. on THz Sci. and Technol., vol. 1, no.1, pp. 220-231, 2011.
[10] S. Skryl, J. B. Jackson, M. I. Bakunov, M. Menu, and G. A. Mourou, "Terahertz time-domain imaging of hidden defects in wooden artworks: application to a Russian icon painting", vol. 53, no. 6, pp. 1033-1038, 2014.
[11] D. Giovannacci, D. Martos-Levif, G.C. Walker, M. Menu, V. Detalle, "Terahertz applications in cultural heritage: case studies", Proc. SPIE, vol. 9065, pp. 906510(7), 2013.
[12] K. Fukunaga, Y. Ogawa, S. Hayashi, I. Hosako, "Terahertz imaging for analysis of historic paintings and manuscripts", Infrared, Millimeter and Terahertz Waves, 33th International Conference on, pp. 1-13, 2008.
[13] J. Labaune, J.B. Jackson, S. Pagès-Camagna, I. N. Duling, M. Menu, G. A. Mourou, "Papyrus imaging with terahertz time domain spectroscopy", Appl. Phys. A, vol. 100, pp. 607-612, 2010.
[14] J. B. Jackson, J. Labaune, G.A. Mourou, L. D'Alessandro, A. Whyte, M. Menu, "Pulsed terahertz investigation of corroded and mineralized copper alloy historical artifacts", Infrared, Millimeter and Terahertz Waves, 36th International Conference on, pp. 1-2, 2011.
[15] I. Cacciari, J. Agresti, S. Siano, "Combined THz and LIPS analysis of corroded archaeological bronzes", Microchem. J., vol. 126, pp. 76-82, 2016.
[16] P. Beckmann, A. Spizzichino, "The Scattering of Electromagnetic Waves from Rough Surfaces", Artech House, London, pp. 80-98, 1987.
[17] S. K. Nayar, K. Ikeuchi, T. Kanade, "Surface reflection: physical and geometrical perspectives", IEEE Trans. Pattern Anal. Machine Intell., vol. 19, no. 7, pp. 611–634, 1991.
[18] T. Fukuchi, N. Fuse, M. Mizuno, K. Fukunaga, "Surface Roughness Measurement Using Terahertz Waves", Proc. 3rd International Conference on Industrial Application Engineering, pp. 294-299, 2015.
[19] M. Herrmann, C. Wiegand, J. Jonuscheit, R. Beigang, "The Influence of Surface Roughness on THz Reflection Measurements", IRMMW-THz 2009, 34th International Conference on Infrared, Millimeter, and Terahertz Waves, pp. 1-2, 2009.
[20] S. Schecklman, L. M. Zurk, S. H. and G. P. Kniffin, "Terahertz material detection from diffuse surface scattering", J. Appl. Phys., vol. 109, no. 9, pp. 094902-1(10), 2011.

[21] C. Jansen, S. Priebem C. Möller, M. Jacob, H. Dierke, M. Koch, T. Kürner, et al., "Diffuse Scattering From Rough Surfaces in THz Communication Channels", IEEE Trans. on Terahertz Science and Technology, vol. 1, no. 2, pp. 462-47, 2011.
[22] Z. Wang, "The influence of surface roughness on conductor at terahertz", Optik, vol. 125, no. 13, pp. 3237-3240, 2014.
[23] T. Fukuchi, N. Fuse, M. Mizuno, and K. Fukunaga, "THz Measurement of Refractive Index and Thickness of Ceramic Coating on a Metal Substrate" Lasers and Electro-Optics Pacific Rim (CLEO-PR), 2013 Conference on, pp. 1-2, 2013.
[24] S. C. Henry, S. Schecklman, G. P. Kniffin, L. M. Zurk, A. Chen, "Measurement and Modeling of Rough Surface Effects on Terahertz Spectroscopy", Proc. of SPIE vol. 7601, pp. 760108-1(10), 2010.
[25] R. Piesiewicz "Scattering Analysis for the Modeling of THz Communication Systems", IEEE Trans. Antennas. Propag. vol. 55, no. 11, pp. 3002-3009, 2007.
[26] I. Cacciari, S. Siano, "THz spectrometer with fiber coupled antennas: Preliminary application test for characterizing stone artefact", Photonics Technologies, pp. 1-4, 2014.
[27] I. Cacciari, D. Ciofini, S. Siano, "THZ characterization of painting layers", Photonics Technologies, pp. 1-4, 2015.
[28] Equivalent roughness values for Surface Finish Grade Numbers is the only data generally available, see f.i. ISO standards 1302:1992.
[29] "Principles of Terahertz Science and Technology", by Yun-Shik Lee, Springer 2009, p. 168.
[30] "Transmission Lines and Networks" by Walter C. Johnson, McGraw-Hill 1963 p. 58.
[31] "Transmission Line Design Handbook "by Brian C Wadell, Artech House 1991 Table 9.3.2 p. 446.
[32] "CRC Handbook of Chemistry and Physics" 1st Student Edition 1998 page F-88.
[33] International Standard ISO 4287. Geometrical Product Specifications (GPS) - surface texture: profile method - terms, definitions and surface texture parameters. Geneva: International Organization for Standardization, 1997.
[34] C.-A. Guérin, "Scattering on rough surfaces with alpha-stable non-Gaussian height distributions", Waves in Random Media, vol. 12, no. 3, pp. 293-306, 2002.
[35] I. Cacciari, P. Nieri, S. Siano, "3D Digital Microscopy for Characterizing Punchworks on Medieval Panel Paintings", J. Comp. and Cult. Herit., vol. 7, no. 4, pp. 1-19, 2015.
[36] I. Cacciari, D. Ciofini, M. Mascalchi, A. Mencaglia, S. Siano "Novel approach to the microscopic inspection during laser cleaning treatments of artworks", Anal. and Bioanal. Chem., vol. 402, no. 4, pp. 1585-1591, 2012.
[37] M. T. Tavassoly, M. Dashtdar, "Height distribution on a rough plane and specularly diffracted light amplitude are Fourier transform pair", Optics Comm., vol. 281, no. 9, 2397-2405, 2008.
[38] I. Cacciari, S. Siano, "THz Characterization of Corroded Metals: The Influence of Surface Roughness", accepted for publication in IET Digital Library 2016.
[39] J. Takayanagi, H. Jinno, S. Ichino, K. Suizu, M. Yamashita, T. Ouchi, S. Kasai, H. Ohtake, H. Uchida, N. Nishizawa, and K. Kawase "High-resolution time-of-flight terahertz tomography using a femtosecond fiber laser", Opt. Exp., vol. 17, no. 9, pp. 7533-7539, 2009.
[40] K. Su, Y.-C. Shen, and J. A. Zeitler, "Terahertz Sensor for Non-Contact Thickness and Quality Measurement of Automobile Paints of Varying Complexity", IEEE Trans. Terahertz Sci. Technol., vol. 4, no. 4, p.432-439, 2014.
[41] J. Chen, Y. Chen, H. Zhao, G. J. Bastiaan, and X.-C. Zhang, "Absorption coefficients of selected explosives and related compounds in the range of 0.1-2.8 THz", Opt. Exp. vol .15, no. 19, pp. 12060-12067, 2007.